$((\eta^5\text{-}C_5H_5)_2Ta(CO)H_2)^+PF_6^-$ (2). A molar solution of HCl (3 mL) was added at room temperature to a suspension of $Cp_2Ta(CO)H$ (1.18 mmol) in water (15 mL) and THF (5 mL). After 0.5 h the mixture was filtered and a solution of NH_4PF_6 (1.23 mmol) in water (5 mL) was added dropwise to the filtrate at 0 °C. The THF was then removed; the white precipitate was filtered, washed with cold water, and dried under vacuum. Crude white solid was obtained 0.45 g, 79% yield. Anal. calcd for $C_{11}H_{12}OF_6PTa$: C, 27.18; H, 2.49. Found: C, 26.92; H, 2.73.

$((\eta^5\text{-}C_5H_4CMe_3)_2Ta(CO)H_2)^+PF_6^-$ (2′). Following the procedure for the preparation of **2** and starting with 200 mg (0.44 mmol) of $(\eta^5\text{-}C_5H_4CMe_3)_2Ta(CO)H$, 190 mg of the crude white solid product **2′** was isolated (72% yield). Anal. Calcd for $C_{19}H_{28}OF_6PTa$: C, 38.14; H, 4.72. Found: C, 38.32; H, 4.86.

$((\eta^5\text{-}C_5H_5)_2Ta(CO)\{HOCH(CH_3)_2\})^+PF_6^-$ (3a). A solution of **2** (1.03 mmol) in CH_3COCH_3 (3 mL) was stirred for 2 h at room temperature. The resulting red solution was then evaporated to dryness. Recrystallization of the crude solid from THF–heptane afforded an analytically pure sample as red crystals (68% yield). Anal. Calcd. for $C_{14}H_{18}O_2F_6PTa$: C, 30.90; H, 3.33. Found: C, 31.05; H, 3.45.

We have carried out another efficient synthesis of this red compound as follows. Acetone (20 mL) and HPF_6 (1 mL of a 60% aqueous solution) was stirred for 0.5 h; 0.6 mL (0.2 mmol) of this solution was added to $Cp_2Ta(CO)H$ (0.2 mmol) dissolved in acetone (10 mL). The color turned immediately from violet to brown-red, and the resulting solution was evaporated. The crude product was then purified as described above.

$((\eta^5\text{-}C_5H_5)_2Ta(CO)\{HOCH(CH_3)(C_2H_5)\})^+PF_6^-$ (3b). The reaction was carried out at room temperature by dissolving compound **2** (0.21 mmol) in $CH_3COC_2H_5$ (2 mL). The mixture was stirred for 1.5 h and evaporated. The crude red solid **2b** was recrystallized from THF–heptane (65% yield). Anal. Calcd for $C_{15}H_{20}O_2F_6PTa$: C, 32.27; H, 3.61. Found: C, 31.94; H, 3.93.

$((\eta^5\text{-}C_5H_5)_2Ta(CO)\{HOCH_2CH_2CH_3\})^+PF_6^-$ (3c). A solution of **2** (0.25 mmol) in CH_3CH_2CHO (2 mL) was stirred for 2 h. The solvent was then removed, and the red solid was purified by recrystallization from THF–heptane (72% yield). Anal. Calcd for $C_{14}H_{18}O_2F_6PTa$: C, 30.90; H, 3.33. Found: C, 30.27; H, 3.91.

$(\eta^5\text{-}C_5H_5)_2Ta(CO)(OCH(CH_3)_2)$ (4a). A molar solution of NaOH was added dropwise to a stirred suspension of **2a** (0.44 mmol) in toluene (10 mL) until a green organic layer was obtained. The toluene layer was decanted and solvent evaporated leading to a green crude solid (53% yield). Mass fragments: *m/e* (assignment, relative intensity) 370 (M^+ – CO, 10), 369 (M^+ – CO – H, 18), 355 ($Cp_2TaOC_2H_4^+$, 18), 341 ($Cp_2TaOCH_2^+$, 5). Anal. Calcd for $C_{14}H_{17}O_2Ta$: C, 42.22; H, 4.30. Found: C, 42.71; H, 4.51.

$(\eta^5\text{-}C_5H_5)_2Ta(CO)(OCH(CH_3)(C_2H_5))$ (4b). Treatment of the salt **3b** (0.09 mmol) with a molar solution of NaOH by the above procedure afforded **4b** as a green solid (48% yield). Mass fragments: *m/e* (assignment, relative intensity) 384 (M^+ – CO, 15), 355 ($Cp_2TaOC_2H_4^+$, 9), 341 ($Cp_2TaOCH_2^+$, 4), 312 (Cp_2TaH^+, 28), 311 (Cp_2Ta^+, 15). Anal. Calcd for $C_{15}H_{19}O_2Ta$: C, 43.70; H, 4.65. Found: C, 44.07; H, 4.43.

$((\eta^5\text{-}C_5H_5)_2Ta(CO)(OCH_2CH_2CH_3)$ (4c). Complex **4c** was prepared (60% yield) by the same method starting from **3c** (0.13 mmol). Mass fragments: *m/e* (assignment, relative intensity) 370 (M^+ – Co, 35), 327 (Cp_2TaO^+, 7), 312 (Cp_2TaH^+, 37), 311 (Cp_2Ta^+, 28). Anal. Calcd for $C_{14}H_{17}O_2Ta$: C, 42.22; H, 4.30. Found: C, 41.88; H, 4.09.

Registry No. **2**, 103241-36-7; **2′**, 103241-38-9; **3a**, 103241-40-3; **3b**, 103241-42-5; **3c**, 103241-44-7; **4a**, 103241-45-8; **4b**, 103241-46-9; **4c**, 103241-47-0; $Cp_2Ta(CO)H$, 11105-69-4; $(\eta^5\text{-}C_5H_4CMe_3)_2Ta(CO)H$, 84749-50-8; CH_3COCH_3, 67-64-1; $CH_3COC_2H_5$, 78-93-3; CH_3CH_2CHO, 123-38-6.

(13) Tebbe, F. N.; Parshall, G. W. *J. Am. Chem. Soc.* **1971**, *93*, 3793.
(14) Reynoud, J. F.; Leblanc, J. C.; Moise, C. *Organometallics* **1985**, *4*, 1059.

He I and He II Photoelectron Spectra and Pseudopotential ab Initio Calculations of Some Tetracoordinated Tin(IV) Derivatives

R. Bertoncello,[1a] J. P. Daudey,[1b] G. Granozzi,*[1a] and U. Russo[1a]

Dipartimento di Chimica Inorganica, Metallorganica ed Analitica, University of Padova, Padova, Italy, and Laboratoire de Physique Quantique, Université Paul Sabatier, Toulouse, France

Received September 17, 1985

The gas-phase UV photoelectron (PE) spectra of $Sn(CH_3)_nCl_{4-n}$ (n = 0–4) and of $Sn(CH_3)_m(NCS)_{4-m}$ (m = 2, 3) are discussed with the aid of the results of pseudopotential ab initio calculations (extended basis sets with inclusion of 5d polarization functions and relativistic corrections for tin). The excellent numerical agreement between experimental and computed (Koopmans) ionization energies has allowed a reassignment of some published PE data and the discussion of the new spectra. The actual involvement of tin 5s, 5p, and 5d atomic orbitals into the valence MOs is also discussed. Both the theoretical and experimental data suggest the presence of strong π_{Sn-Cl} interactions with significant contribution from Sn 5d AOs. As far as the NCS derivatives are concerned, both PE and theoretical data are in agreement with a largely ionic bond.

Introduction

The electronic structures of many organotin compounds have been studied extensively by means of gas-phase UV photoelectron spectroscopy.[2-10] Up to now, however, the assignment of the various PE bands has been accomplished mainly by using experimental criteria. Among them, however, He I vs. He II intensity changes have rarely aided the interpretation of the PE spectra of tin compounds. In

(1) (a) University of Padova. (b) Université P. Sabatier, Toulouse.
(2) Green, J. C.; Green, M. L. H.; Joachim, P. J.; Orchard, A. F.; Turner, D. W. *Philos. Trans. R. Soc. London, A* **1970**, *268*, 111.
(3) Evans, S.; Green, J. C.; Joachim, P. J.; Orchard, A. F. *J. Chem. Soc., Faraday Trans. 2* **1972**, *2*, 905.
(4) Boschi, R.; Lappert, M. F.; Pedley, J. B.; Schmidt, W.; Wilkins, B. T. *J. Organomet. Chem.* **1973**, *50*, 69.
(5) Flamini, A.; Semprini, E.; Stefani, F.; Sorriso, S.; Cardaci, G. *J. Chem. Soc., Dalton Trans.* **1976**, 731.
(6) Cauletti, C.; Furlani, C.; Piancastelli, M. N. *J. Organomet. Chem.* **1978**, 149, 289.
(7) Egdell, R. G.; Fragalà, I.; Orchard, A. F. *J. Electron Spectrosc.* **1979**, *17*, 267.
(8) Fragalà, I.; Ciliberto, E.; Egdell, R. G.; Granozzi, G. *J. Chem. Soc., Dalton Trans.* **1980**, 145.
(9) Bancroft, G. M.; Pellach, E.; Tse, J. S. *Inorg. Chem.* **1982**, *21*, 2950.
(10) Fragalà, I.; Ciliberto, E.; Finocchiaro, P.; Recca, A. *J. Chem. Soc., Dalton Trans.* **1979**, 240.

0276-7333/86/2305-1866$01.50/0

Table I. Pseudopotential ab Initio Results for $Sn(CH_3)_4$[a]

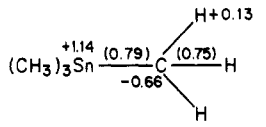

MO	IE calcd[b]	IE exptl[c]	% pop. Sn s	Sn p	Sn d	4 C	12 H	dominant character
$3t_2$ (HOMO)	9.49	9.70 (A)		20	1	70	9	Sn–C bonding MO
$1t_1$	13.01					55	45	
1e	13.55	13.40 (B)			1	52	47	CH_3-based MOs
$2t_2$	13.59			4		53	43	
$2a_1$	14.48		39			49	12	Sn(5s)–C

[a] Gross atomic charges and overlap populations (in parentheses) are in electrons. [b] Values rescaled by nine tenths; energies in eV. [c] Experimental values from ref 3.

fact, the qualitative use in the UV region of the Gelius model[11] for the photoionization cross sections (CSs) has been prevented by the lack of unambiguous experimental evidence about Sn 5p intensity changes on passing from He I to He II radiation. Recently, in our laboratory, this problem has been settled by definitive evidence from the He I and He II spectra of the $Sn_2(CH_3)_6$ molecule.[12]

From the theoretical point of view, rigorous quantum mechanical calculations on molecules containing such heavy atoms have been discouraged, up to now, by the large number of core electrons which increases abnormally the dimensions of the secular determinant. Therefore, a valuable tool for UV–PE band assignments, namely, the comparison with theory, has been limited to those few cases where semiempirical[13] or MS-Xα[14] calculations have been employed. At present, however, the availability of pseudopotential ab initio methods enables us to perform rigorous quantum mechanical calculations with relatively low effort. In previous studies we have shown that this method is very accurate in reproducing the UV–PE data of several organotin derivatives.[12,15] This approach also can be used to answer quantitatively some open questions concerning the bonding in organotin compounds, such as the actual involvement of tin 5s, 5p, and 5d atomic orbitals (AOs) in the valence molecular orbitals (MOs).

With these two methods in hand, i.e., the He I/He II experimental criterion and the ab initio theoretical method, we decided to rediscuss the PE band assignments and the electronic structures of the $Sn(CH_3)_nCl_{4-n}$ (n = 0–4) series. Extended basis set ab initio calculations, including 5d polarization functions and relativistic pseudopotentials for tin, have been carried out on the whole series, whereas He I/He II PE spectra have been recorded when necessary to complete the literature data. Moreover, the PE spectra and calculations on $Sn(CH_3)_m(NCS)_{4-m}$ (m = 2, 3) have been reported and discussed for the first time.

Experimental Section

UV–PE Spectra. Samples used for PE measurements were either commercial ($SnCH_3Cl_3$) or prepared according to literature methods[16] ($Sn(CH_3)_3NCS$ and $Sn(CH_3)_2(NCS)_2$). He I and He II gas-phase PE spectra were recorded on a Perkin-Elmer PS 18 spectrometer modified for He II measurements by inclusion of a hollow cathode discharge lamp that gives a high photon flux at He II wavelengths (Helectros Developments). The spectrometer was connected on-line with a Minc-23 computer (Digital Equipment) by an interface built in our laboratory. Data acquisition was carried out by several sweeps (4–8) over 500 distinct channels. Typical sweep time amounts to 5–10 min. The ionization energy (IE) scale was calibrated by reference to peaks due to admixed inert gases (Xe, Ar) and to the He $1s^{-1}$ self-ionization. The reported IEs are the mean values over several distinct runs. For convenience of the discussion, literature and reported PE bands have been alphabetically labeled.

Calculations. The ab initio LCAO–MO–SCF calculations were performed with the introduction of pseudopotentials to deal with all core electrons using the formalism proposed by Durand and co-workers.[17] The reported pseudopotential for tin includes the major relativistic corrections[17] (mass and Darwin corrections). 3-1G split Gaussian basis sets[15,18] were optimized for each valence shell of C, N, S, and Sn by a pseudopotential version of the ATOM program,[19] whereas for H the standard Huzinaga Gaussian basis set[20] has been 3+1 contracted. 5d polarization functions (ξ = 0.20) have been added for the tin atom.[21] All the molecular calculations were carried out by running the PSHONDO program[22] on a VAX 730 (DEC) computer. The geometrical parameters adopted in the calculations for the $Sn(CH_3)_nCl_{4-n}$ compounds were derived from the gas-phase electron diffraction results[23,24] because of the well-known tendency of tetracoordinated Sn compounds to give pentacoordination or even linear polymers in the solid state. As far as the $Sn(CH_3)_3NCS$ and $Sn(CH_3)_2(NCS)_2$ compounds are concerned, for which no gas-phase structure determination was available, we have idealized the published X-ray solid-state results,[25,26] respectively to C_{3v} and C_{2v} symmetric structures assuming tetrahedral bond angles, while the reported bond distances are maintained. The arbitrariness of this choice is reflected in the poorer matching between theoretical and experimental IEs in these two cases with respect to $Sn(CH_3)_nCl_{4-n}$ ones. Gross atomic charges and bond overlap populations (OPs) were obtained by Mulliken's population analysis.[27]

(11) Gelius, U. In *Electron Spectroscopy*; Shirley, D. A., Ed.; North Holland Publishing: Amsterdam 1972; pp 311–334.
(12) Granozzi, G.; Bertoncello, R.; Tondello, E.; Ajó, D. *J. Electron Spectrosc.* **1985**, *36*, 207.
(13) Armstrong, D. R.; Perkins, P. G. *Coord. Chem. Rev.* **1981**, *31*, 139.
(14) Zhu, J.-K.; Li, D.; Li, J.; Pan, Y.-K. *Theor. Chim. Acta (Berlin)* **1983**, *63*, 223.
(15) Cauletti, C.; Furlani, C.; Granozzi, G.; Sebald, A.; Wrackmeyer, B. *Organometallics* **1985**, *4*, 290.
(16) (a) Seyferth, D.; Rochow, E. G. *J. Am. Chem. Soc.* **1955**, *77*, 1302. (b) Wada, M.; Nichima, N.; Ikawara, R. *J. Organomet. Chem.* **1965**, *3*, 70.
(17) (a) Barthelat, J. C.; Durand, P.; Serafini, A. *Mol. Phys.* **1977**, *33*, 159. (b) Barthelat, J. C.; Pelissier, M.; Durand, P. *Phys. Rev. A* **1981**, *21*, 1773.
(18) (a) Daudey, J. P.; Jeung, G.; Ruiz, M. E.; Novaro, O. *Mol. Phys.* **1982**, *46*, 87. (b) Ruiz, M. E.; Daudey, J. P.; Novaro, O. *Mol. Phys.* **1982**, *46*, 853.
(19) Roos, B.; Salez, C.; Veillard, A.; Clementi, E. A General Program for Calculation of Atomic SCF Orbitals by the Expansion Method; Technical Report RJ 518, IBM Research, 1968.
(20) Huzinaga, S. *J. Chem. Phys.* **1965**, *42*, 1293.
(21) Fernandez, J.; Arriau, J.; Dargelos, A. *Chem. Phys.* **1985**, *94*, 397.
(22) Daudey, J. P., A Modified Version of HONDO Program (Dupuis, M.; Rys, J.; King, M. F. *QCPE* **1900**, *336*) Including Pseudopotentials.
(23) Skinner, H. A.; Sutton, L. E. *Trans. Faraday Soc.* **1944**, *40*, 164.
(24) Beagley, B.; McAloon, K.; Freeman, J. M. *Acta Cryst.* **1974**, *B30*, 444.
(25) Chow, Y. M. *Inorg. Chem.* **1970**, *9*, 794.
(26) Forder, R. A.; Sheldrick, G. M. *J. Organomet. Chem.* **1970**, *21*, 115.

Table II. Pseudopotential ab Initio Results for $SnCl_4$[a]

$$Cl_3Sn\overset{+0.92\ (0.69)\ -0.23}{\text{———}}Cl$$

MO	IE calcd[b]	IE exptl[c]	% pop. Sn s	Sn p	Sn d	4 Cl	dominant character
$1t_1$ (HOMO)	12.14	12.10 (A)				100	Cl lone pairs
$3t_2$	12.38	12.38, 12.50 (B)		2	4	94	Cl lone pairs
1e	12.79	12.71 (C)			3	97	Cl lone pairs
$2t_2$	14.05	14.00 (D)		20		80	Sn–Cl bonding MO
$2a_1$	17.24	17.00 (E)	40			60	Sn(5s)–Cl

[a] Gross atomic charges and overlap populations (in parentheses) are in electrons. [b] Values rescaled by nine tenths; energies in eV. [c] Experimental values from ref 2.

Table III. Pseudopotential ab Initio Results for $Sn(CH_3)_3Cl$[a]

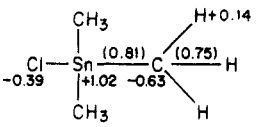

MO	IE calcd[b]	IE exptl[c]	% pop. Sn s	Sn p	Sn d	Cl	3 C	9 H	dominant character
5e (HOMO)	9.87	9.90 (A)		14	2	22	56	6	Sn–C bonding MO
4e	11.17	11.31 (B)		9	1	75	13	2	Cl lone pair
$5a_1$	11.36		1	13	2	63	17	4	Sn–Cl bonding MO
$1a_2$	13.62	13.80 (C)					55	45	CH_3-based MOs
3e	13.81			1		1	54	44	CH_3-based MOs
2e	14.06			4			54	42	CH_3-based MOs
$4a_1$	14.21			4		2	51	43	CH_3-based MOs
$3a_1$	15.20	15.24 (C′)	39			18	34	9	Sn(5s)–C, Sn(5s)–Cl

[a] Gross atomic charges and overlap populations (in parentheses) are in electrons. [b] Values rescaled by nine tenths; energies in eV. [c] Experimental values from ref 8.

UV-PE and Theoretical Results

In the following we will critically examine the UV-PE assignments in the light of the quantum mechanical results singly for each compound. An excellent matching between calculated (within the Koopmans' theorem[28]) and experimental IEs is obtained when the eigenvalues are rescaled by nine tenths in the whole studied series. The same kind of agreement has been obtained for other tin derivatives,[12,15] indicating that Koopmans' theorem holds for these classes of compounds. On the other hand, the 10% rescaling probably reflects the limitations of the used basis set.

$Sn(CH_3)_4$. The He I excited PE spectrum of $Sn(CH_3)_4$ has been already reported by Green et al.[3] while the He II intensities have been discussed by Bancroft et al.[9] The theoretical results of Table I confirm the previous assignments which relate the first band, centered at 9.70 eV, to the ionization from the $3t_2$ σ_{Sn-C} bonding MO and the second band, centered at 13.4 eV, to $1t_1$, 1e, $2t_2$ (σ_{C-H} bonding), and $2a_1$ (Sn–C bonding) ionizations. The eigenvector analysis allows us to evaluate the involvement of the Sn AOs in the various MOs; from Table I it emerges that the tin 5p contribution to the $3t_2$ MO amounts to 20% only, a value rather small when compared to that predicted by Bancroft et al.[9] (30–40%). Moreover, in previous work[12] we pointed out that the Sn 5p PE CSs will decrease with respect to C 2p and will increase with respect to H 1s CSs when passing from He I to He II radiation. With these data in hand, the observed increase of the intensity ratio between the first and the second band under He II radiation may be ascribed to a dominant C 2p contribution to $3t_2$ MO and to a concomitant 43–47% H 1s contribution to $1t_1$, 1e, and $2t_2$ MOs rather than to a Sn 5p effect.

$SnCl_4$. The He I PE spectrum of $SnCl_4$ has been reported and interpreted by Green et al.,[2] while the He II spectrum has been discussed in two different papers.[7,9]

Theoretical results reproduce quantitatively the experimental IEs, and the interpretative pattern that emerges is in complete agreement with the literature[2,7,9] (Table II); the splitting of band B, associated with spin–orbit coupling of the tetrahedrally disposed chlorine atoms, cannot be reproduced by our theoretical approach since the spin–orbit coupling operator is not included in the Hamiltonian and no other semiempirical method has been adopted in order to evaluate this spin–orbit splitting.

An interesting feature that emerges from the eigenvector analysis is the involvement of the Sn 5d AOs that, for symmetry reasons, contribute only to MOs of t_2 and e irreducible representations. In particular, the Cl 3p lone pairs ($3t_2$ and 1e MOs) show a nonnegligible contribution from the 5d Sn AOs which lead them to acquire a small Sn–Cl bonding character (in 1e only π in nature). The small contribution of Sn 5p AOs to the $3t_2$ MO (2.0%) is in agreement with Bancroft's calculation[9] (1.6% calculated by Xα-SW method).

$Sn(CH_3)_3Cl$ The He I and He II PE spectra of $Sn(CH_3)_3Cl$ have been reported by Fragalá et al.,[8] while, in a previous paper, Flamini et al.[5] have discussed only the He I spectrum. The excellent matching between calculated and experimental IEs (Table III) allows us to propose with confidence some slightly different assignments. In agreement with the previous assignment, we associate band A to ionization from the 5e MO (σ_{Sn-C} bonding). The subsequent band B, previously related to the ionization from an e-type MO, is to be associated with ionizations

(27) Mulliken, R. S. *J. Chem. Phys.* **1955**, *23*, 1833.
(28) Koopmans, T. C. *Physica (Amsterdam)* **1934**, *1*, 104.

Table IV. Pseudopotential ab Initio Results for $Sn(CH_3)_2Cl_2$[a]

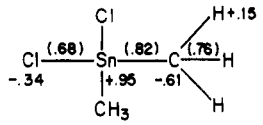

MO	IE calcd[b]	IE exptl[c]	% pop. Sn s	Sn p	Sn d	2 Cl	2 C	6 H	dominant character
$4b_1$ (HOMO)	10.25	10.43 (A)		13	2	29	51	5	Sn–C bonding MO
$6a_1$	11.12		1	6	3	70	18	2	
$4b_2$	11.12	11.31 (B)		1	1	98			Cl lone pairs
$2a_2$	11.37			1		98		1	
$3b_1$	12.06			15		65	16	4	
$5a_1$	12.21	12.16 (C)		14	1	68	13	4	Sn–Cl bonding MOs
$3b_2$	12.38			13	2	79	3	3	
$2b_1$	14.33			2		1	54	43	
$1a_2$	14.33	14.30 (D)			1		55	44	CH_3-based MOs
$4a_1$	14.59			3		1	54	42	
$2b_2$	14.64			4		4	51	41	
$3a_1$	15.90	15.93 (D′)	40			33	20	7	Sn(5s)–C, Sn(5s)–Cl

[a] Gross atomic charges and overlap populations (in parentheses) are in electrons. [b] Values rescaled by nine tenths; energies in eV. [c] Experimental values from ref 8.

from both the 4e and $5a_1$ MOs. The former, as it results from the eigenvector analysis, represents a combination of Cl 3p lone pair AOs with some π_{Sn-Cl} bonding contribution, while the latter ($5a_1$) represents a σ_{Sn-Cl} (and to a smaller extent Sn–C) bonding interaction. The next broad band C is related to ionizations from $1a_2$, 3e, 2e, and $4a_1$ MOs (σ_{C-H} bonding), while the higher IE shoulder C′ pertains to the inner $3a_1$ MO (Sn–C bonding with minor Sn–Cl bonding character) with a large Sn 5s AO contribution (39%). The He II spectrum confirms these assignments; in particular, the relative intensity decrease of band B with respect to bands A and C must be related to the lowering of Cl 3p CSs at He II wavelengths compared to C 2p and Sn 5p ones.

Finally, the theoretical results provide strong evidence in favor of a significant mixing between π_{Cl} lone pairs and the σ_{Sn-C} bonds. Actually, the overlap population analysis of 5e and 4e MOs shows that the former presents some Sn–Cl antibonding character whereas the latter gains some Sn–C bonding character. A similar σ/π mixing between σ_{Sn-C} and $\pi_{C\equiv C}$ e-type MOs has been already found in analogous $Sn(CH_3)_3$–alkynyl compounds.[15]

$Sn(CH_3)_2Cl_2$. The He I and He II PE spectra of $Sn(CH_3)_2Cl_2$ have been discussed by Cauletti et al.[6] and by Fragalà et al.[8] Similarly to the previous case, we suggest some different assignments of the PE data. We agree with the assignments of band A and band B to ionizations from one MO ($4b_1$, σ_{Sn-C} bonding) and three MOs ($6a_1$, $4b_2$, $2a_2$) (Table IV), respectively. The eigenvector analysis shows that the three MOs related to band B are mainly Cl 3p lone pairs; among them, however, the $6a_1$ MO presents significant Sn and C AOs participation (10 and 18%, respectively) which gives rise to a σ_{Sn-C} bonding character. At variance with the literature assignment, we propose to relate the next band C to ionization from three MOs ($3b_1$, $5a_1$, $3b_2$). The $3b_1$ MO represents a Cl 3p lone pair with π_{Sn-Cl} bonding contribution, while the $5a_1$ and $3b_2$ MOs show a predominant σ_{Sn-Cl} bonding character. It is noteworthy that the Sn–Cl π interaction shifts the fourth Cl lone pair ($3b_1$ MO) toward the IE region peculiar to the Sn–Cl σ bonds. Band D is related to ionizations from four σ_{C-H} bonding levels ($2b_1$, $1a_2$, $4a_1$, $2b_2$), while its higher IE shoulder D′ pertains to the ionization of the $3a_1$ MO with a 40% contribution of Sn 5s AO.

The He II spectrum[8] confirms these assignments and the theoretical results: the intensity increase of band A with respect to bands B and C at He II wavelengths reflects the predominant C 2p population (51%) of the related $4b_1$ MO; on the other hand, band B decreases with respect to band C according to the larger Cl 3p populations of the corresponding MOs.

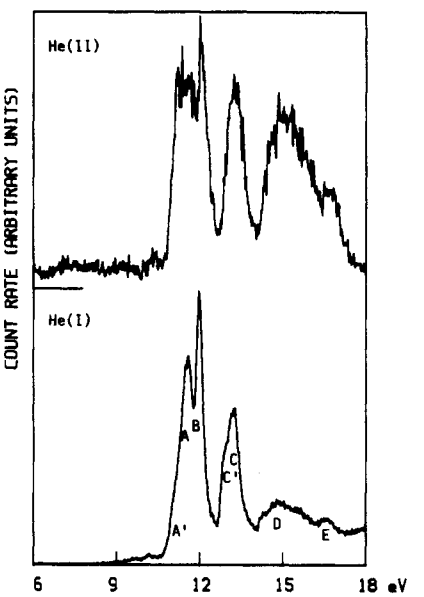

Figure 1. He I and He II excited PE spectra of $SnCH_3Cl_3$.

$SnCH_3Cl_3$. The He I and He II PE spectra of $SnCH_3Cl_3$ are reported in Figure 1. Only a short account of the general features of the He(I) spectrum can be found in the literature.[29] The quantum mechanical ab initio calculation together with the proposed assignments is reported in Table V.

The lowest IE feature (shoulder A′) must be related to ionization from the σ_{Sn-C} bonding $5a_1$ MO. The next bands A and B represent ionizations from chlorine lone pairs: in particular, the excellent agreement between theoretical and experimental IEs makes us confident in assigning band A to ionization from $1a_2$ and 5e MOs and band B to ionization from 4e MO. A small Sn–Cl bonding character is found in 4e and 5e MOs because of a nonnegligible Sn 5d involvement. Shoulder C′ must be related to ionization from a MO ($4a_1$) which originates from a Cl lone pair with

(29) Stocco, G. C.; Orchard, A. F. *Chim. Ind. (Milan)* **1977**, *59*, 122.

Table V. Pseudopotential ab Initio Results for $SnCH_3Cl_3$[a]

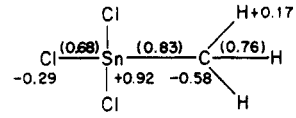

MO	IE calcd[b]	IE exptl[c]	% pop. Sn s	Sn p	Sn d	3 Cl	C	3 H	dominant character
$5a_1$ (HOMO)	11.12	11.18 (A′)	1	8	3	53	31	4	Sn–C bonding MO
$1a_2$	11.58	11.59 (A)				100			Cl lone pairs
5e	11.71	11.65 (A)		1	2	97			
4e	12.10	12.01 (B)		1	3	96			
$4a_1$	13.04	12.93 (C′)		20		64	14	2	
3e	13.22	13.25 (C)		16	1	78	3	2	Sn–Cl bonding MO
2e	15.04	14.86 (D)		3		4	53	40	CH_3-Based MO
$3a_1$	16.59	16.62 (E)	40			48	9	3	Sn(5s)–C, Sn(5s)–Cl

[a] Gross atomic charges and overlap populations (in parentheses) are in electrons. [b] Values rescaled by nine tenths; energies in eV. [c] Experimental values from Figure 1.

Table VI. Pseudopotential ab Initio Results for $Sn(CH_3)_3NCS$[a]

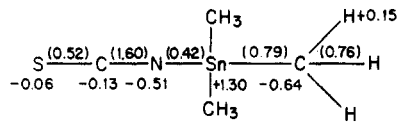

MO	IE calcd[b]	IE exptl[c]	% pop. Sn s	Sn p	Sn d	N	C	S	3 CH_3	dominant character
6e (HOMO)	8.24	8.73 (A)		1		23	1	72	3	π_S lone pair
5e	10.23	10.45 (B)		22	1		3	3	71	Sn–C bonding MO
4e	13.11	12.39 (C)		1		47	39	10	3	$\pi_{N=C}$ bonding MO
$7a_1$	13.18	12.71 (C)	9	5	1	16	11	27	31	Sn–C bonding MO
$1a_2$	13.83								100	CH_3-based MOs
3e	14.01	13.55 (D′)		1		1	1		97	
$6a_1$	14.03		9			2	13	41	35	σ_S lone pair
2e	14.21	14.08 (D)		3		1			96	CH_3-based MOs
$5a_1$	14.45		9	5		1	1	3	81	
$4a_1$	17.89	16.80 (E)	15	4		56	10	5	10	Sn(5s)–N bonding MO

[a] Gross atomic charges and overlap populations (in parentheses) are in electrons. [b] Values rescaled by nine tenths; energies in eV. [c] Experimental values from Figure 2.

both Sn–Cl and Sn–C bonding character, while band C represents ionization from a 3e σ_{Sn-Cl} bonding MO. The subsequent broad envelope, labeled D, is assigned to a 2e σ_{C-H} bonding MO, while the next weak band E represents the ionization from the $3a_1$ MO, prevalently Sn–Cl bonding in character, with a 40% contribution of Sn AOs (entirely 5s).

The most striking evidence of the He II spectrum consists of the large intensity increase of shoulder A′ with respect to bands A and B, as expected from the different AOs contribution to the corresponding MOs (see Table V). Analogously, the intensity increase of band D can be viewed in the light of C 2p contributions to the 2e MO. The He II intensity increase of band E (assigned to the $3a_1$ MO) with respect to bands A, B, and C can be interpreted by assuming that Sn 5s AO CS behaves similarly to the Sn 5p CSs on going from He I to He II radiation; i.e., it increases with respect to Cl 3p AOs, but it decreases with respect to C 2p AOs. Analogous conclusions can be drawn from the He I/He II relative intensity variations of the related shoulders D′ in the $Sn(CH_3)_2Cl_2$ and $Sn(CH_3)_3Cl$ compounds.[8]

$Sn(CH_3)_3NCS$. The He I and He II PE spectra of $Sn(CH_3)_3NCS$ are reported in Figure 2, while the pseudopotential ab-initio calculation results[30] are presented in

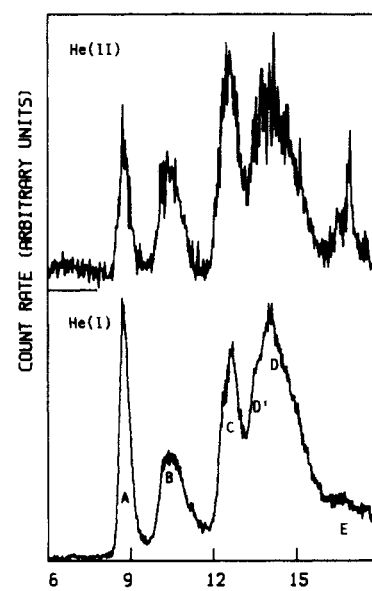

Figure 2. He I and He II excited PE spectra of $Sn(CH_3)_3NCS$.

Table VI. The low IE region (up to 10.00 eV) presents a sharp band, labeled A, to be assigned to the ionization from the 6e MO (NCS π MO, mainly localized on sulfur). The following band B represents the ionization from the 5e MO of σ_{Sn-C} bonding character. Band C must be associated with two MOs (4e and $7a_1$); the 4e MO represents

(30) Remember that the crystal state structure[26] shows that both Sn–N–C and N–C–S bond angles are very close to 180° (173 (5)° and 175 (6)°, respectively).

Table VII. Pseudopotential ab Initio Results for $Sn(CH_3)_2(NCS)_2$[a]

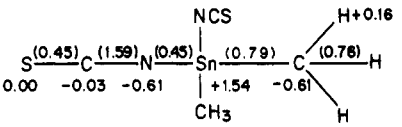

MO	IE calcd[b]	IE exptl[c]	% pop. Sn s	Sn p	Sn d	2 N	2 C	2 S	2 CH_3	dominant character
$5b_2$ (HOMO)	8.70			1		22	1	71	5	
$7b_1$	8.70	9.18 (A)		1		23	1	75		S lone pairs
$3a_2$	8.74					23	2	75		
$9a_1$	8.84			1		22	2	75		
$4b_2$	10.93	11.10 (B)		23	1		4	6	66	Sn–C bonding MOs
$8a_1$	12.88		11	7	2	21	13	9	37	
$6b_1$	13.26					49	39	11		
$2a_2$	13.33	13.00 (C)				50	39	10	1	$\pi_{N=C}$ bonding MOs
$3b_2$	13.51			4		48	35	8	5	
$7a_1$	13.61		2	5		44	30	10	9	
$5b_1$	14.06			2		10	24	60	4	σ_S lone pairs
$6a_1$	14.43	13.90 (D′)	6	1		2	22	59	10	
$2b_2$	14.64			2		1	1		96	
$1a_2$	14.65					1			99	CH_3-Based MOs
$4b_1$	14.81	14.50 (D)		2		1	2	4	93	
$5a_1$	14.89		2	3				1	94	
$3b_1$	17.65			10	1	65	13	10	1	Sn–N bonding MO
$4a_1$	19.28		20	2		54	11	6	7	Sn(5s)–N

[a] Gross atomic charges and overlap populations (in parentheses) are in electrons. [b] Values rescaled by nine tenths; energies in eV. [c] Experimental values from Figure 3.

$\pi_{N=C}$ bond, while the $7a_1$ MO shows a σ_{Sn-C} bonding character with some σ_{C-S} and σ_{N-C} antibonding contribution. It is important to note that the $7a_1$ MO does not carry any Sn–N bonding character. The large separation between 4e and 5e MOs (experimentally 1.94 eV) does not allow any mixing between the $\pi_{N=C}$ MOs of the NCS moiety and the σ_{Sn-C} MO of the $Sn(CH_3)_3$ moiety, at variance with the case of $Sn(CH_3)_3Cl$. The experimental shift of the Sn–C band (B) toward higher IE with respect to the analogous band of $Sn(CH_3)_3Cl$ is indicative of a stronger electron withdrawal of the NCS fragment with respect to the Cl atom (see the tin gross atomic charges in Tables III and VI). Shoulder D′ and band D must be related to ionizations from a series of five MOs: four of them are σ_{C-H} bonding levels ($1a_2$, 3e, 2e, $5a_1$), while the remaining one ($6a_1$) is mainly localized on the sulfur atom (essentially a σ lone pair with C–S antibonding character). Incidentally, the low value of the S–C overlap population (see Table VI) is to be attributed to the antibonding contribution originating from this $6a_1$ MO.

The last low-intensity band E represents ionization from a σ_{Sn-N} bonding MO ($4a_1$). In a way similar to the previous cases, the Sn contribution to this inner MO comes prevalently from 5s AO. At variance with the chlorine derivatives, where several MOs contribute to the Sn–Cl bond using Sn 5p AOs, in $Sn(CH_3)_3NCS$ derivative only the $4a_1$ MO shows a Sn–N bonding character. This fact suggests a large ionic character of the Sn–N bond, in agreement with analogous conclusions drawn from the $Sn(CH_3)_3$–alkynyl compounds.[15]

The He II spectrum confirms the previous assignments when, as reported in the literature,[31] a large intensity decrease of S 3p CSs and an intensity increase of N 2p ones on going from He I to He II radiation are assumed. In particular, band A shows a large relative intensity decrease while the opposite is true for bands C and E.

$Sn(CH_3)_2(NCS)_2$. The He I and He II PE spectra of $Sn(CH_3)_2(NCS)_2$ are reported in Figure 3, while the ab initio pseudopotential results are presented in Table VII.

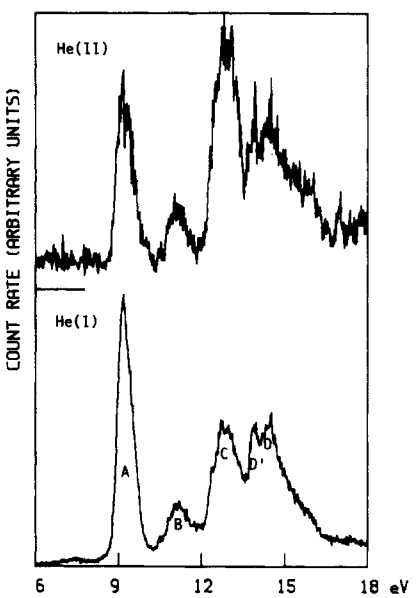

Figure 3. He I and He II excited PE spectra of $Sn(CH_3)_2(NCS)_2$.

Band A must be related to the ionization from four MOs ($5b_2$, $7b_1$, $3a_2$, $9a_1$), prevalently S lone pairs; the sharpness of this band and the comparison with the PE spectrum of $Sn(CH_3)_3NCS$ well suit with this assignment. The next band B, on the basis of its low intensity, is assigned to ionization from a bonding MO with prevalent σ_{Sn-C} bonding character.

The assignment of the C, D′, and D bands can be accomplished mostly on the basis of the theoretical results. Band C, then, is assigned to ionization from five MOs, the first of which ($8a_1$) represents the second σ_{Sn-C} bonding MO while the remaining four ($6b_1$, $2a_2$, $3b_2$, $7a_1$) pertain to $\pi_{N=C}$ bonding MOs. The next bands D′ and D are assigned to the ionization from six MOs, the first two ($5b_1$, $6a_1$) being mainly localized on the sulfur atoms (σ_S lone pairs with C–S antibonding character), while the remaining four ($2b_2$, $1a_2$, $4b_1$, $5a_1$) pertain to the σ_{C-H} bonding levels.

(31) Schweig, A.; Thiel, W. *J. Chem. Phys.* **1974**, *60*, 951.

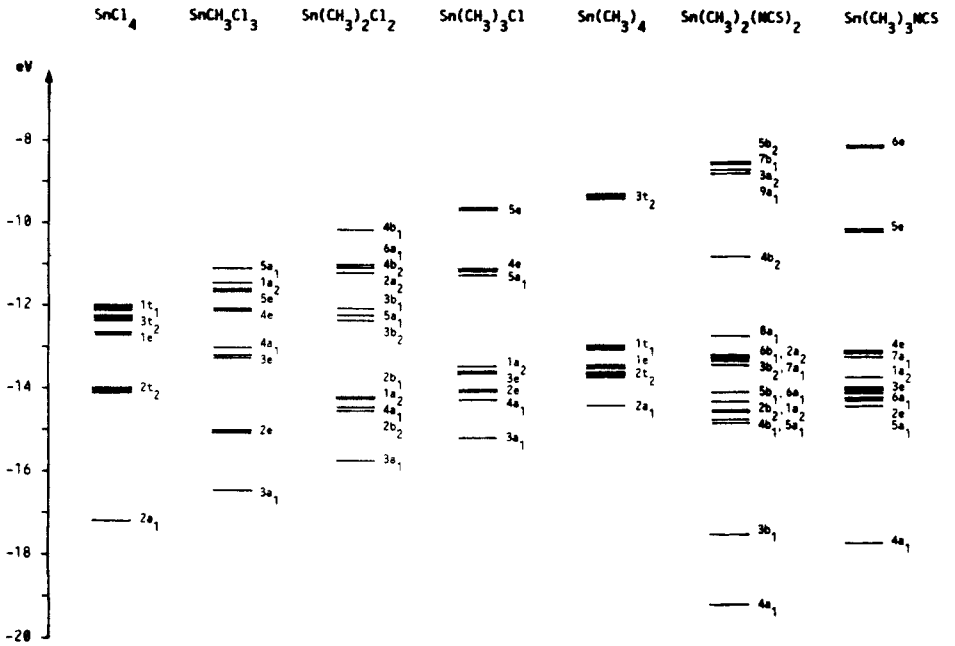

Figure 4. Calculated valence energy levels for $Sn(CH_3)_nCl_{4-n}$ (n = 0–4) and $Sn(CH_3)_m(NCS)_{4-m}$ (m = 2, 3).

Table VIII. Atomic and/or Fragment Charges According to Mulliken Population Analysis of the ab Initio Eigenvectors of the Studied Molecules

		$SnCl_4$	$SnCH_3Cl_3$	$Sn(CH_3)_2Cl_2$	$Sn(CH_3)_3Cl$	$Sn(CH_3)_4$	$Sn(CH_3)_2(NCS)_2$	$Sn(CH_3)_3NCS$
Sn	s	1.06	1.09	1.09	1.06	1.00	0.96	1.02
	p	1.58	1.62	1.66	1.69	1.69	1.33	1.51
	d	0.44	0.37	0.30	0.23	0.17	0.17	0.17
	net	+0.92	+0.92	+0.95	+1.02	+1.14	+1.54	+1.30
CH_3			−0.07	−0.16	−0.21	−0.28	−0.12	−0.20
Cl		−0.23	−0.29	−0.34	−0.39			
NCS							−0.64	−0.70

The He II spectrum shows an intensity decrease of band A, while band C and, to a lesser extent, band B show increased relative intensities. The AO contributions to the various MOs account for this behavior: in particular, the relative lowering of band A in the He II spectrum reflects S 3p contributions to the related MOs, while the higher relative intensity of band C at He II wavelength can be related to N 2p contributions to the associated MOs. Furthermore, the intensity growth of band B in the He II spectrum is associated with the predominant C 2p contribution (64%) in the related MO. The examination of the He II intensities within bands D′ and D does not provide any further hint about the energy ordering of the related six MOs.

Conclusions

To summarize the electronic structure trends that emerge from this study, we report in Figure 4 a correlation diagram of the calculated valence energy levels.

Let us focus our attention primarily on the trends in the $Sn(CH_3)_nCl_{4-n}$ series. The progressive substitution of chlorine atoms by methyl groups produces a destabilization of all the valence MOs, as expected on the basis of the higher electronegativity of the chlorine atoms. A similar trend emerges from a XPS study reported by Jolly and Avanzino[32] where the tin $3d_{5/2}$ core binding energies were observed along the same series. In particular, if we adopt the empirical method proposed by Jolly[33] to relate shifts of core binding energies with shifts of nonbonding valence IEs (i.e., valence shifts $\simeq {}^{8}/_{10}$ of core shifts) and choose as a reference the innermost a_1-type Sn 5s based MO (in all molecules the Sn 5s contribution is 39–40%), we obtain a quantitative agreement between the XPS and UPS (and theoretical) results.

On the other hand, the trend of the tin gross atomic charges along the series (as obtained by the Mulliken population analysis and reported in Table VIII) does not agree with simple electronegativity arguments. In fact, we observe that the successive replacement of chlorine atoms by methyl groups induces a monotonic increase in the negative charge on both Cl and methyl, with the former in all cases retaining the larger negative charge. Since the increases in the negative charge on methyl are larger than those on Cl, there is a concomitant increase in the positive charge on Sn.

In our opinion, this finding substantiates the idea that has been suggested by the eigenvector analysis of the reported calculations: the Sn–Cl bonding interaction possesses a certain degree of π character, in part due to the involvement of Sn 5d functions in the bonding. Actually the Sn 5d population in the series (Table VIII) gradually increases by an amount of 0.07e/chlorine atom. Analogous conclusions concerning the role of the Sn 5d AOs in the $p_\pi \rightarrow d_\pi$ bonding were drawn by Jolly[34] from XPS data of the tetrahalides of Si, Ge, and Sn. An analogous π $CH_3 \rightarrow Sn_{5d}$ bonding is probably discouraged by both overlap and energy matching reasons.

As far as the NCS derivatives, we observe that NCS exherts an electron-withdrawing effect much stronger than chlorine, so that the compounds are as a whole much more

(32) Avanzino, S. C.; Jolly, W. L. *J. Electron Spectrosc.* **1976**, *8*, 15.
(33) Jolly, W. L. *Acc. Chem. Res.* **1983**, *16*, 370.
(34) Jolly, W. L. *Chem. Phys. Lett.* **1983**, *100*, 546.

ionic (see the tin gross atomic charges). The involvement of the Sn 5d functions is comparable with the small one found in $Sn(CH_3)_4$, owing, in this case, too, to the scarce energy matching between the Sn 5d AOs and the suitable $\pi_{N=C}$ MOs.

Acknowledgment. Thanks are due to CNR (ROME) for a financial support to this study.

Registry No. $Sn(CH_3)_4$, 594-27-4; $SnCl_4$, 7646-78-8; $Sn(CH_3)_3Cl$, 1066-45-1; $Sn(CH_3)_2Cl_2$, 753-73-1; $SnCH_3Cl_3$, 993-16-8; $Sn(CH_3)_3NCS$, 15597-43-0; $Sn(CH_3)_2(NCS)_2$, 15768-03-3.

Reaction of a Diiron μ-Methylidyne Complex with 1,2-Disubstituted Alkenes

Charles P. Casey,* Mark W. Meszaros, Seth R. Marder, Ruta K. Bly, and Paul J. Fagan

McElvain Laboratories of Organic Chemistry, Department of Chemistry, University of Wisconsin, Madison, Wisconsin 53706

Received February 3, 1986

Reaction of $[(C_5H_5)(CO)Fe]_2(\mu\text{-}CO)(\mu\text{-}CH)^+PF_6^-$ (**1**) with *cis*-2-butene produced a 2.3:1.0:1.5 equilibrium mixture of $[(C_5H_5)(CO)Fe]_2(\mu\text{-}CO)(\mu\text{-}CCH(CH_3)CH_2CH_3)^+PF_6^-$ (**2**) and two isomers of $[(C_5H_5)(CO)Fe]_2(\mu\text{-}CO)(\mu\text{-}\eta^1,\eta^2\text{-}CH{=}C(CH_3)CH_2CH_3)^+PF_6^-$ (**3**-*E* and **3**-*Z*) in 79% yield. Reaction of this equilibrium mixture with $NaHCO_3$ produced $[(C_5H_5)(CO)Fe]_2(\mu\text{-}CO)(\mu\text{-}C{=}C(CH_3)CH_2CH_3)$ (**8**) in 80% yield. Reaction of **1** with *trans*-2-butene, cyclohexene, cyclopentene, *trans*-1-propenylbenzene, and *trans*-2-pentene gave similar equilibrium mixtures of μ-alkylidyne and μ-alkenyl complexes which are deprotonated to produce μ-alkylidene complexes. The reaction of **1**-*d* with *cis*-2-butene gave **2**-*d* and **3**-*d* with the deuterium label located on the methylene group of the ethyl group. This result provides conclusive evidence that μ-alkylidyne complexes are the kinetic products in the reaction of **1** with 1,2-disubstituted alkenes. Direct observation of a μ-alkylidyne complex by low-temperature NMR supports this conclusion.

The cationic diiron μ-methylidyne complex $[(C_5H_5)(CO)Fe]_2(\mu\text{-}CO)(\mu\text{-}CH)^+PF_6^-$ (**1**) reacts with alkenes to form new carbon–carbon bonds and produces either μ-alkylidyne or μ-alkenyl complexes.[1-5] With terminal alkenes, the methylidyne C–H bond adds regioselectively across the alkene carbon–carbon double bond. Both the relative reactivity of alkenes toward **1** and the observation of an inverse isotope effect on the addition of **1**-*d* to alkenes are consistent with a transition state for μ-alkylidyne formation that involves only carbon–carbon bond formation as shown in I. After the transition state has been reached, a 1,3-hydride shift (possibly from a carbocation intermediate) completes the addition of the C–H unit to the alkene. The transition state for this 1,3-hydride shift is depicted as II.

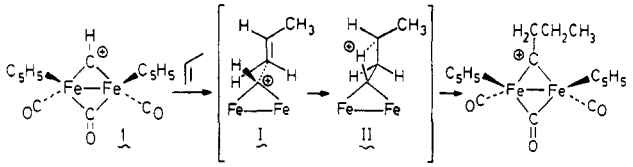

Some alkenes such as 1-methylcyclohexene, 1,1-diphenylethylene, and 2,3,3-trimethyl-1-butene react with methylidyne complex **1** to produce μ-alkenyl complexes directly. In general, more highly substituted alkenes capable of forming stabilized carbocation intermediates tend to lead directly to μ-alkenyl products. The inverse secondary isotope effect seen in the reaction of 2,3,3-trimethyl-1-butene is consistent with a transition state for μ-alkenyl formation that involves only carbon–carbon bond formation.[5] The resulting carbocation intermediate then undergoes a 1,2-hydrogen or 1,2-carbon shift via transition state III to complete the formation of the μ-alkenyl complex

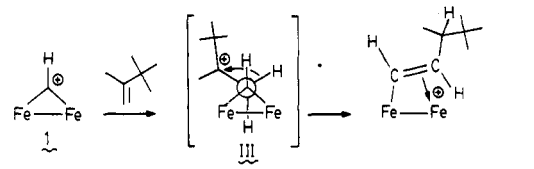

The transition states for the rate-determining step of μ-alkylidyne and μ-alkenyl formation are very similar and involve only carbon–carbon bond formation. The partitioning of the cationic intermediate between μ-alkylidyne and μ-alkenyl complexes is determined largely by steric effects which affect the relative energies of the product-determining transition states II and III.

When we first observed that *cis*-2-butene and other 1,2-disubstituted alkenes reacted with **1** to produce mixtures of μ-alkylidyne and μ-alkenyl complexes, we proposed that these products were formed directly from **1** by competing pathways.[6] However, we subsequently discovered that μ-alkylidyne complexes with two carbon substituents on the carbon α to the carbyne center undergo rapid and reversible 1,2-hydride shifts to form an equilibrium mixture of μ-alkylidyne and μ-alkenyl complexes.[7] In this paper we present two independent lines of evidence that establish that the reaction of **1** with *cis*-2-butene and other 1,2-disubstituted alkenes occurs via kinetic formation of

(1) Casey, C. P.; Fagan, P. J.; Miles, W. H. *J. Am. Chem. Soc.* **1982**, *104*, 1134–1136.
(2) Casey, C. P.; Fagan, P. J. *J. Am. Chem. Soc.* **1982**, *104*, 4950–4951.
(3) Casey, C. P.; Fagan, P. J.; Miles, W. H.; Marder, S. R. *J. Mol. Catal.* **1983**, *21*, 173–188.
(4) Casey, C. P.; Meszaros, M. W.; Fagan, P. J.; Bly, R. K.; Marder, S. R.; Austin, E. A. *J. Am. Chem. Soc.* **1986**, *108*, 4043–4053.
(5) Casey, C. P.; Meszaros, M. W.; Fagan, P. J.; Bly, R. K.; Colborn, R. E. *J. Am. Chem. Soc.* **1986**, *108*, 4053–4059.
(6) Casey, C. P.; Meszaros, M. W.; Marder, S. R.; Fagan, P. J. *J. Am. Chem. Soc.* **1984**, *106*, 3680–3681.
(7) (a) Casey, C. P.; Marder, S. R.; Fagan, P. J. *J. Am. Chem. Soc.* **1983**, *105*, 7197–7198. (b) Casey, C. P.; Marder, S. R.; Adams, B. R. *J. Am. Chem. Soc.* **1985**, *107*, 7700–7705 and references therein.

0276-7333/86/2305-1873$01.50/0